Supporting Information

Binding of Human ACE2 and RBD of Omicron Enhanced by Unique Interaction Patterns Among SARS-CoV-2 Variants of Concern

Seonghan Kim[1], Yi Liu[1], Matthew Ziarnik[1], Sangjae Seo[2], Yiwei Cao[3], X. Frank Zhang[1,4*], Wonpil Im[1,3*]

[1]Department of Bioengineering, [2]Korean Institute of Science and Technology Information, Daejeon 34141, Republic of Korea, [3]Departments of Biological Sciences, Chemistry, and Computer Science and Engineering, Lehigh University, 111 Research Dr, Bethlehem, PA 18015, USA
[4]Current address: Department of Biomedical Engineering, University of Massachusetts Amherst, 240 Thatcher Road, Amherst, MA 01003, USA

[*]Correspondence and requests for materials should be addressed to X.F.Z and W.I. (emails: frank.zhang@umass.edu and wonpil@lehigh.edu)

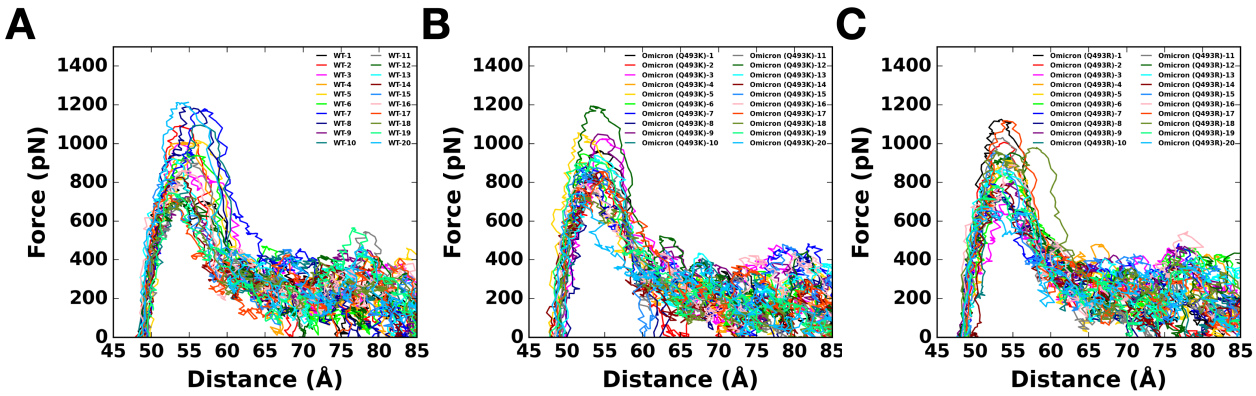

Figure S1. Force profiles of 20 replicas of (A) WT, (B) Omicron Q493K, and (C) Omicron Q493R as a function of the distance between the COM of RBD and ACE2.

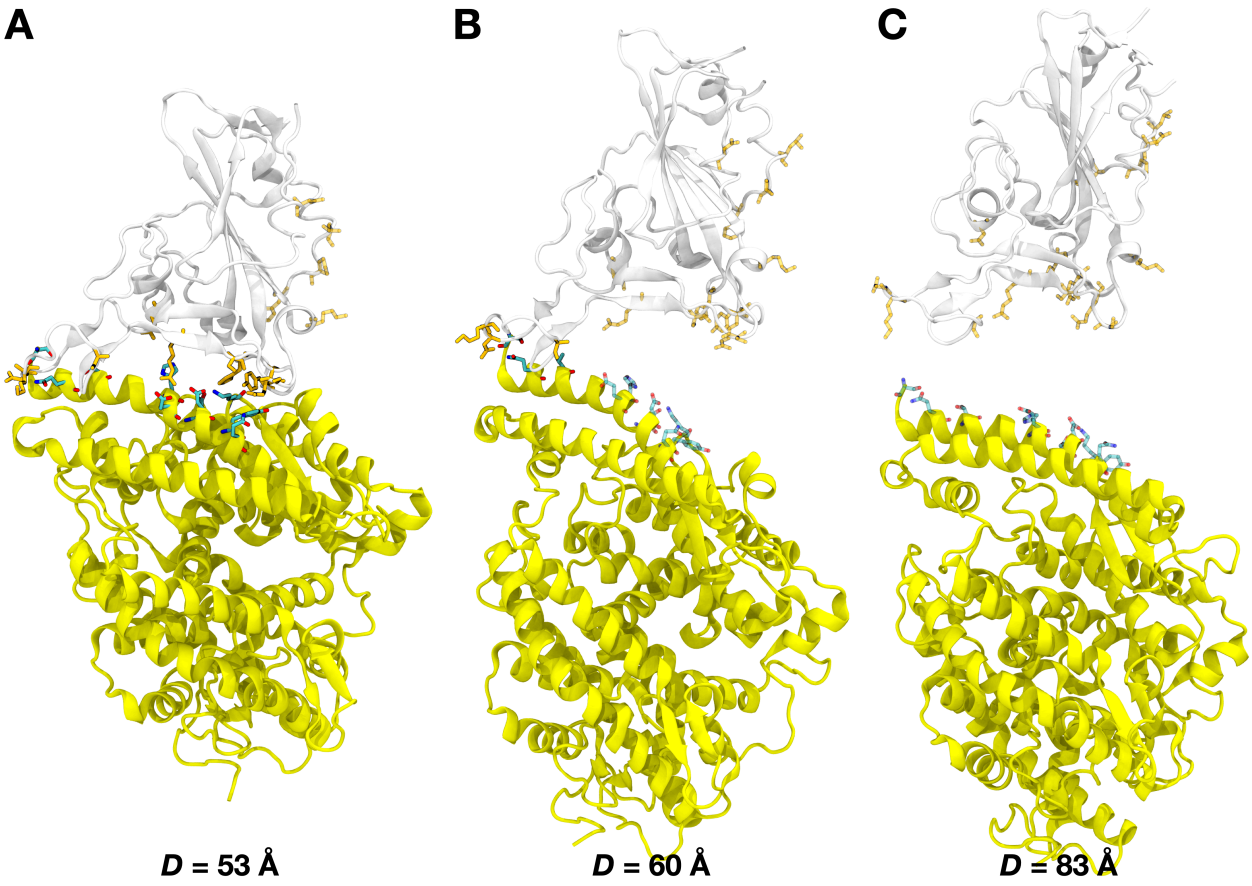

Figure S2. Separation process between Omicron RBD and ACE2 at *D* = 53 Å, 60 Å, and 83 Å, respectively. The color scheme is the same as in **Figure 1B**.

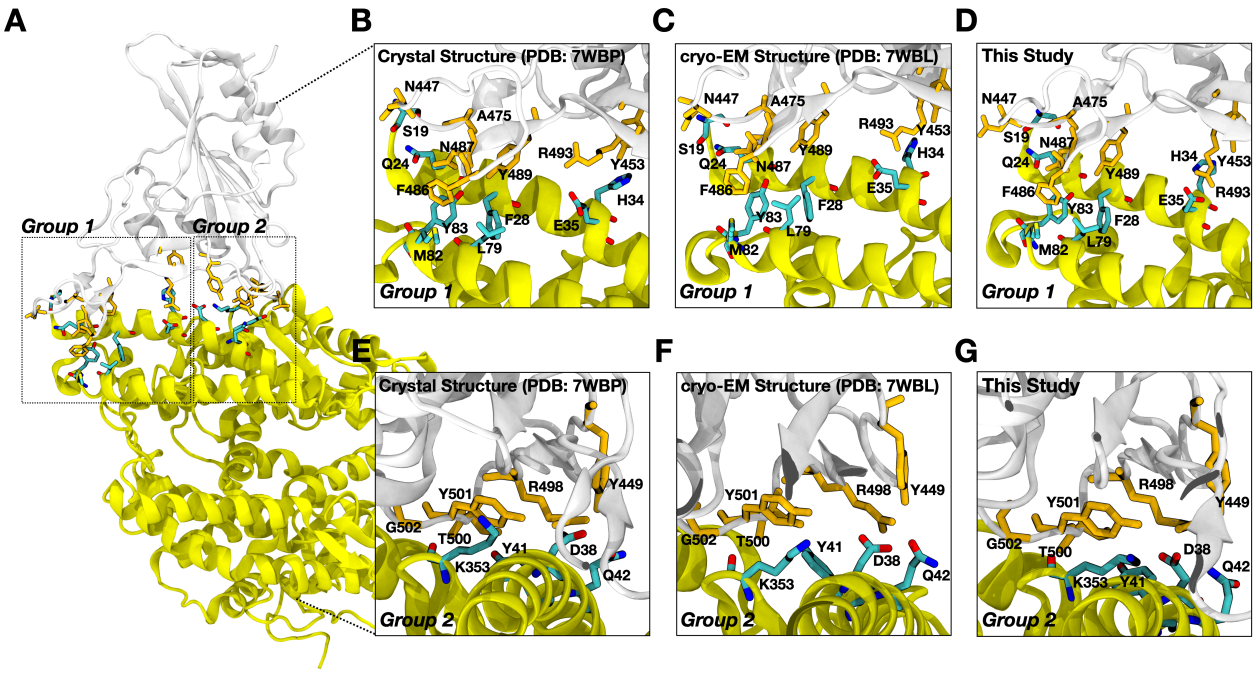

Figure S3. Model comparisons between experimentally obtained structures from (B,E) X-ray crystallography (PDB ID: 7WBP), (C,F) cryo-EM (PDB ID: 7WBL), and (D,G) the model used in this work. Residues located in the RBD^{Omicron}-ACE2 interface are compared. (A) Two groups are defined and magnified on the right: (B,C,D) for group 1 and (E,F,G) for group2. The color scheme is the same as in **Figure 1B**.

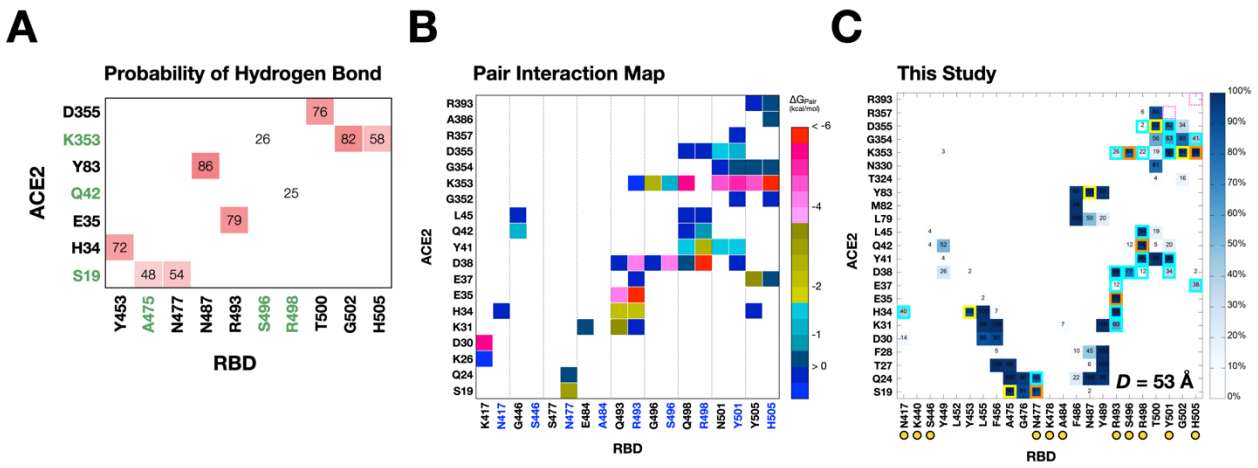

Figure S4. Comparison of interaction maps between Omicron RBD and ACE2. **(A)** Probability of hydrogen bonds obtained from 100 ns of simulations started from Omicron RBD cryo-EM structure (PDB ID: 7T9L). The figure was regenerated from the study conducted by Hossen et al.[1], where the unique interfacial hydrogen bonds found in Omicron are colored in green on the X- and Y-axes. **(B)** Pair interaction map from 500 ns of simulations started after Omicron mutation based on WT RBD X-ray structure (PDB ID: 6M0J). The figure was reproduced from the study by Jawad et al.[2] The residues colored in blue on the X-axis are Omicron residues, and residues colored in black are WT. **(C)** The interaction map from this study. The yellow boxes represent interactions reported by Hossen et al. in **(A)**, the cyan boxes present interactions reported by Jawad et al. in **(B)**, and the orange boxes are interactions reported in both studies. Dotted magenta boxes represent missing weak interactions shown in **(B)**. Interactions reported by Hossen et al. were fully captured. Note that **(A)** and **(B)** show RBD residues only subjected to mutation in Omicron, while **(C)** provides more interaction information caused by key interacting RBD residues in addition to mutated residues addressed in the previous two studies.

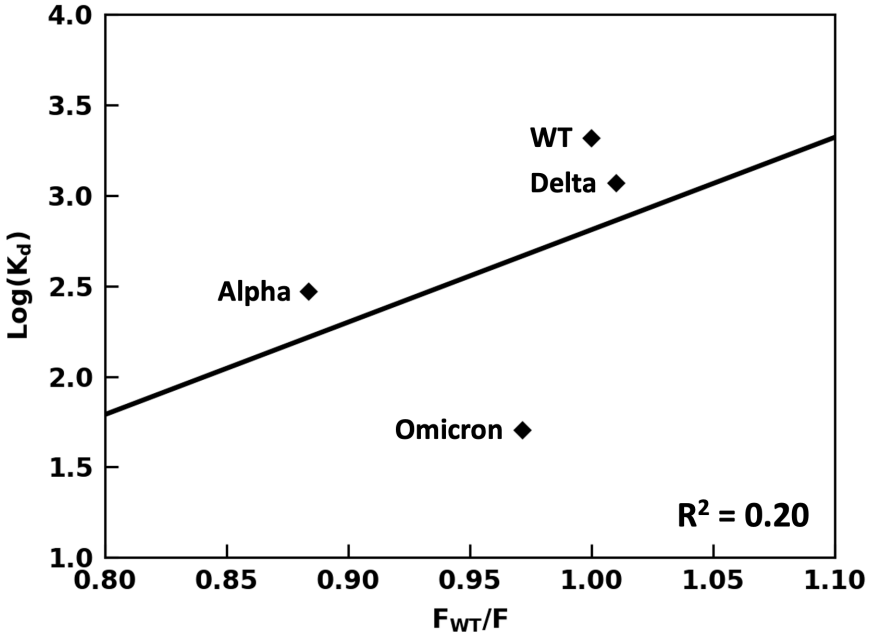

Figure S5. Linear regression between MST experiments ($\log(K_d)$) and SMD simulations (F_{WT}/F). The F_{WT}/F is a ratio, where F_{WT} and F are the maximum pulling forces of WT and all variants (Alpha, Delta, and Omicron Q493R) from our SMD simulations.

Table S1. Comparison of the affinities in K_d (nM) reported in the current study and other reported in the literature. Abbreviations: SPR, surface plasmon resonance; BLI, biolayer interferometry.

References	WT	Alpha	Beta	Delta	Omicron
This study	27.5	11.8	23.1	21.5	5.50
ref[3] (SPR)	8.30	-	-	-	-
ref[4] (SPR)	24.6	5.40	13.8	25.1	31.4
ref[5] (SPR)	26.3	3.64	8.10	-	-
ref[6] (SPR)	44.2	-	-	-	-
ref[7] (BLI)	58.8	20.8	-	-	-
ref[8] (SPR)	62.6	5.50	17.4	-	-
ref[9] (SPR)	68.3	-	-	-	24.4
ref[10] (BLI)	75.1	10.7	-	-	-
ref[11] (SPR)	5.92	-	-	-	2.80
ref[12] (SPR)	-	-	7.35	2.85	8.85
ref[13] (SPR)	58.6	9.56	24.9	-	25.7
ref[14] (SPR)	7.30	1.50	3.20	4.90	7.80

REFERENCES

(1) Hossen, M. L.; Baral, P.; Sharma, T.; Gerstman, B.; Chapagain, P. Significance of the RBD mutations in the SARS-CoV-2 omicron: from spike opening to antibody escape and cell attachment. *Phys. Chem. Chem. Phys.* **2022**, *24*, 9123-9129.

(2) Jawad, B.; Adhikari, P.; Podgornik, R.; Ching, W. Y. Binding Interactions between Receptor-Binding Domain of Spike Protein and Human Angiotensin Converting Enzyme-2 in Omicron Variant. *J. Phys. Chem. Lett.* **2022**, *13*, 3915-3921.

(3) Tian, F.; Tong, B.; Sun, L.; Shi, S.; Zheng, B.; Wang, Z.; Dong, X.; Zheng, P. N501Y mutation of spike protein in SARS-CoV-2 strengthens its binding to receptor ACE2. *Elife* **2021**, *10*.

(4) Han, P.; Li, L.; Liu, S.; Wang, Q.; Zhang, D.; Xu, Z.; Han, P.; Li, X.; Peng, Q.; Su, C.; Huang, B.; Li, D.; Zhang, R.; Tian, M.; Fu, L.; Gao, Y.; Zhao, X.; Liu, K.; Qi, J.; Gao, G. F.; Wang, P. Receptor binding and complex structures of human ACE2 to spike RBD from omicron and delta SARS-CoV-2. *Cell* **2022**, *185*, 630-640 e610.

(5) Han, P.; Su, C.; Zhang, Y.; Bai, C.; Zheng, A.; Qiao, C.; Wang, Q.; Niu, S.; Chen, Q.; Zhang, Y.; Li, W.; Liao, H.; Li, J.; Zhang, Z.; Cho, H.; Yang, M.; Rong, X.; Hu, Y.; Huang, N.; Yan, J.; Wang, Q.; Zhao, X.; Gao, G. F.; Qi, J. Molecular insights into receptor binding of recent emerging SARS-CoV-2 variants. *Nat. Commun.* **2021**, *12*, 6103.

(6) Shang, J.; Ye, G.; Shi, K.; Wan, Y.; Luo, C.; Aihara, H.; Geng, Q.; Auerbach, A.; Li, F. Structural basis of receptor recognition by SARS-CoV-2. *Nature* **2020**, *581*, 221-224.

(7) Lee, J. H.; Lee, Y.; Lee, S. K.; Kim, J.; Lee, C. S.; Kim, N. H.; Kim, H. G. Versatile role of ACE2-based biosensors for detection of SARS-CoV-2 variants and neutralizing antibodies. *Biosens. Bioelectron.* **2022**, *203*, 114034.

(8) Barton, M. I.; MacGowan, S. A.; Kutuzov, M. A.; Dushek, O.; Barton, G. J.; van der Merwe, P. A. Effects of common mutations in the SARS-CoV-2 Spike RBD and its ligand, the human ACE2 receptor on binding affinity and kinetics. *Elife* **2021**, *10*.

(9) Cui, Z.; Liu, P.; Wang, N.; Wang, L.; Fan, K.; Zhu, Q.; Wang, K.; Chen, R.; Feng, R.; Jia, Z.; Yang, M.; Xu, G.; Zhu, B.; Fu, W.; Chu, T.; Feng, L.; Wang, Y.; Pei, X.; Yang, P.; Xie, X. S.; Cao, L.; Cao, Y.; Wang, X. Structural and functional characterizations of infectivity and immune evasion of SARS-CoV-2 Omicron. *Cell* **2022**, *185*, 860-871 e813.

(10) Supasa, P.; Zhou, D.; Dejnirattisai, W.; Liu, C.; Mentzer, A. J.; Ginn, H. M.; Zhao, Y.; Duyvesteyn, H. M. E.; Nutalai, R.; Tuekprakhon, A.; Wang, B.; Paesen, G. C.; Slon-Campos, J.; Lopez-Camacho, C.; Hallis, B.; Coombes, N.; Bewley, K. R.; Charlton, S.; Walter, T. S.; Barnes, E.; Dunachie, S. J.; Skelly, D.; Lumley, S. F.; Baker, N.; Shaik, I.; Humphries, H. E.; Godwin, K.; Gent, N.; Sienkiewicz, A.; Dold, C.; Levin, R.; Dong, T.; Pollard, A. J.; Knight, J. C.; Klenerman, P.; Crook, D.; Lambe, T.; Clutterbuck, E.; Bibi, S.; Flaxman, A.; Bittaye, M.; Belij-Rammerstorfer, S.; Gilbert, S.; Hall, D. R.; Williams, M. A.; Paterson, N. G.; James, W.; Carroll, M. W.; Fry, E. E.; Mongkolsapaya, J.; Ren, J.; Stuart, D. I.; Screaton, G. R. Reduced neutralization of SARS-CoV-2 B.1.1.7 variant by convalescent and vaccine sera. *Cell* **2021**, *184*, 2201-2211 e2207.

(11) Lan, J.; He, X.; Ren, Y.; Wang, Z.; Zhou, H.; Fan, S.; Zhu, C.; Liu, D.; Shao, B.; Liu, T.-Y.; Wang, Q.; Zhang, L.; Ge, J.; Wang, T.; Wang, X. *bioRxiv* **2022**.

(12) Zhang, X.; Wu, S.; Wu, B.; Yang, Q.; Chen, A.; Li, Y.; Zhang, Y.; Pan, T.; Zhang, H.; He, X. SARS-CoV-2 Omicron strain exhibits potent capabilities for immune evasion and viral entrance. *Signal Transduct. Target Thers.* **2021**, *6*, 430.

(13) Cameroni, E.; Bowen, J. E.; Rosen, L. E.; Saliba, C.; Zepeda, S. K.; Culap, K.; Pinto, D.; VanBlargan, L. A.; De Marco, A.; di Iulio, J.; Zatta, F.; Kaiser, H.; Noack, J.; Farhat, N.; Czudnochowski, N.; Havenar-Daughton, C.; Sprouse, K. R.; Dillen, J. R.; Powell, A. E.; Chen, A.; Maher, C.; Yin, L.; Sun, D.; Soriaga, L.; Bassi, J.; Silacci-Fregni, C.; Gustafsson, C.; Franko, N. M.; Logue, J.; Iqbal, N. T.; Mazzitelli, I.; Geffner, J.; Grifantini, R.; Chu, H.; Gori, A.; Riva, A.; Giannini, O.; Ceschi, A.; Ferrari, P.; Cippa, P. E.; Franzetti-Pellanda, A.; Garzoni, C.; Halfmann, P. J.; Kawaoka, Y.; Hebner, C.; Purcell, L. A.; Piccoli, L.; Pizzuto, M. S.; Walls, A. C.; Diamond, M. S.; Telenti, A.; Virgin, H. W.; Lanzavecchia, A.; Snell, G.; Veesler, D.; Corti, D. Broadly neutralizing antibodies overcome SARS-CoV-2 Omicron antigenic shift. *Nature* **2022**, *602*, 664-670.
(14) Dejnirattisai, W.; Huo, J.; Zhou, D.; Zahradnik, J.; Supasa, P.; Liu, C.; Duyvesteyn, H. M. E.; Ginn, H. M.; Mentzer, A. J.; Tuekprakhon, A.; Nutalai, R.; Wang, B.; Dijokaite, A.; Khan, S.; Avinoam, O.; Bahar, M.; Skelly, D.; Adele, S.; Johnson, S. A.; Amini, A.; Ritter, T. G.; Mason, C.; Dold, C.; Pan, D.; Assadi, S.; Bellass, A.; Omo-Dare, N.; Koeckerling, D.; Flaxman, A.; Jenkin, D.; Aley, P. K.; Voysey, M.; Costa Clemens, S. A.; Naveca, F. G.; Nascimento, V.; Nascimento, F.; Fernandes da Costa, C.; Resende, P. C.; Pauvolid-Correa, A.; Siqueira, M. M.; Baillie, V.; Serafin, N.; Kwatra, G.; Da Silva, K.; Madhi, S. A.; Nunes, M. C.; Malik, T.; Openshaw, P. J. M.; Baillie, J. K.; Semple, M. G.; Townsend, A. R.; Huang, K. A.; Tan, T. K.; Carroll, M. W.; Klenerman, P.; Barnes, E.; Dunachie, S. J.; Constantinides, B.; Webster, H.; Crook, D.; Pollard, A. J.; Lambe, T.; Consortium, O.; Consortium, I. C.; Paterson, N. G.; Williams, M. A.; Hall, D. R.; Fry, E. E.; Mongkolsapaya, J.; Ren, J.; Schreiber, G.; Stuart, D. I.; Screaton, G. R. SARS-CoV-2 Omicron-B.1.1.529 leads to widespread escape from neutralizing antibody responses. *Cell* **2022**, *185*, 467-484 e415.